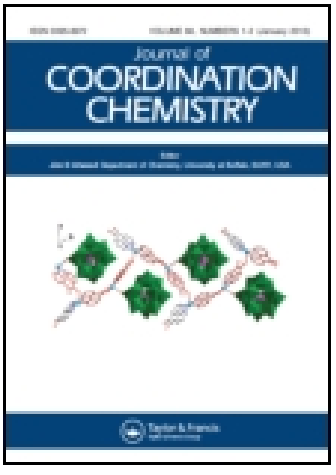

Journal of Coordination Chemistry
Publication details, including instructions for authors and subscription information:
http://www.tandfonline.com/loi/gcoo20

Syntheses, crystal structures, and electrochemical studies of $Fe_2(CO)_6(\mu\text{-}PPh_2)(\mu\text{-}L)$ (L = OH, $OPPh_2$, PPh_2)

Yao-Cheng Shi[a], Wei Yang[a], Ying Shi[a] & Da-Cong Cheng[a]
[a] College of Chemistry and Chemical Engineering, Yangzhou University, Yangzhou, PR China

Accepted author version posted online: 04 Jul 2014.Published online: 07 Aug 2014.

Journal of Coordination Chemistry, 2014
Vol. 67, No. 13, 2330–2343, http://dx.doi.org/10.1080/00958972.2014.940925

Syntheses, crystal structures, and electrochemical studies of $Fe_2(CO)_6(\mu\text{-}PPh_2)(\mu\text{-}L)$ (L = OH, $OPPh_2$, PPh_2)

YAO-CHENG SHI*, WEI YANG, YING SHI and DA-CONG CHENG

College of Chemistry and Chemical Engineering, Yangzhou University, Yangzhou, PR China

(*Received 31 March 2014; accepted 4 June 2014*)

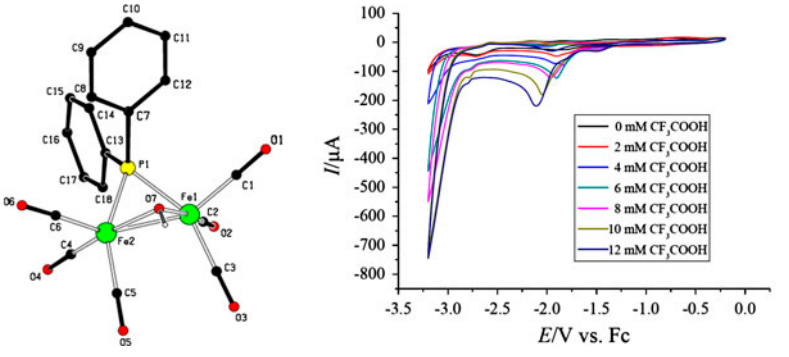

Reaction of $Fe_3(CO)_{12}$ and Ph_2PH in the presence of Et_3N in THF at 0 °C immediately forms $Fe_2(CO)_6(\mu\text{-}PPh_2)(\mu\text{-}OH)$ (**1**), $Fe_2(CO)_6(\mu\text{-}PPh_2)(\mu\text{-}k^2O,P\text{-}OPPh_2)$ (**2**), and $Fe_2(CO)_6(\mu\text{-}PPh_2)_2$ (**3**) in yields of 25, 14, and 19%, respectively. Experiments confirm that Et_3N shortens the reaction time. The absence of O_2 hinders the formation of **2**. The presence of H_2O can increase the yield of **1**. Their structures have been determined by X-ray crystallography and the complexes have been completely characterized by EA, IR, and ^1H, ^{13}C, ^{31}P NMR. Electrochemical studies reveal that they exhibit catalytic H_2-producing activities.

Keywords: Iron–iron bond; Bridging hydroxyl group; Carbonyl ligand; Hydrogenase

1. Introduction

Designing catalytic systems based on inexpensive and abundant materials is vital to the development of a hydrogen energy economy [1–4]. However, few examples of platinum-free electrode materials capable of catalyzing proton reduction have appeared [5]. Recently, chemists have favored syntheses of organometallic complexes inspired by hydrogenase enzymes [6–11]. Considerable interest was focused on diiron thiolates $[Fe_2(\mu\text{-}SRS)(CO)_{6-n}L_n]$

*Corresponding author. Email: ycshi@yzu.edu.cn

(R = linking group, L = σ-donating ligand), because of their structural resemblance with the catalytic site of [Fe–Fe] hydrogenases. Advances in biomimetic modeling were derived from the studies of substituted compounds (L = cyanide, isocyanide, phosphine, carbene, phenanthroline), which protonate to produce well-characterized hydrides [12]. Dinuclear iron(I) complexes with thiolate-bridges were shown to catalyze the electrochemical reduction of protons to molecular hydrogen in organic solvents [13, 14]. Studies were extended to the possible role of a heteroatom (N, O, or S) as a proton relay in the bridging ligand [15–20]. Aside from possibly participating in the heterolytic formation and cleavage of hydrogen, the bridging ligand plays a key role in controlling the electron-transfer processes [13]. Since proton reduction catalysis by all CO diiron models (except aza-bridged derivatives) is initiated by a reduction step [21–23], broadening the range of bridging ligands should include increasing the chemical reversibility of the reduction step and decreasing the reduction potential of the diiron complex [24–27]. However, to date, comparatively few electrochemical studies have examined the effect of replacing sulfur with other donors in (Fe_2(μ-NRN) [28, 29], Fe_2(μ-PRP) [18, 30, 31], Fe_2(μ-SeRSe) [32–35], and Fe_2(μ-TeRTe) [34]). Best and coworkers [30, 31] demonstrated that phosphide-bridged derivatives undergo a reversible single-step two-electron reduction leading to proton reduction catalysis at rather negative potentials. Selenolate-bridged diiron complexes were shown to exhibit mostly irreversible reduction processes analogous to that observed for related thiolate compounds with bridging ligand having an alkyl group [32, 33]. With few examples of Fe_2(μ-PPh_2) complexes [36], we decided to carry out the syntheses, crystal structures, and electrochemistry of diiron complexes with bridging PPh_2. As the structures differ significantly from the well-characterized Fe_2(μ-SRS) motifs, we felt that they will extend hydrogenase models to catalyze proton reduction.

2. Experimental

2.1. *Materials and physical measurements*

All reactions were carried out under a prepurified N_2 atmosphere with standard Schlenk techniques. All solvents were dried by refluxing over appropriate drying agents and stored under an N_2 atmosphere. THF was distilled from sodium-benzophenone, petroleum ether (60–90 °C), and CH_2Cl_2 from P_2O_5. $Fe_3(CO)_{12}$ [37] and Ph_2PH [38] were prepared according to literature procedures. The progress of all reactions was monitored by TLC (silica gel H, 300-400 mesh). NMR spectra were carried out on a Bruker Avance 600 spectrometer using TMS as an internal standard or 85% H_3PO_4 as an external standard in $CDCl_3$. IR spectra were recorded on a Bruker Tensor 27 spectrometer as KBr disks from 400 to 4000 cm^{-1}. Analyses for C and H were performed on a Vario EL microanalyzer. Melting points were measured on a Yanagimoto apparatus and are uncorrected. Electrochemical determinations were carried out on a CHI66OD potentiostat.

2.2. *Reaction of $Fe_3(CO)_{12}$, Ph_2PH, S, and Et_3N with PhCOCl*

A 100-mL Schlenk flask equipped with a stir bar and serum cap was charged with 15 mL of THF, 0.376 g (2 mM) of Ph_2PH, and 0.064 g (2 mM) of elemental sulfur. After 30 min, to this solution was added 0.28 mL (2 mM) of Et_3N and 2 g (4 mM) of $Fe_3(CO)_{12}$. After

30 min, to this solution was added 0.23 mL (2 mM) of PhCOCl. After stirring for 24 h, the solvent was removed under reduced pressure and the resulting residue was chromatographed by TLC on silica gel. Elution with petroleum ether/CH_2Cl_2 (v/v, 1 : 2) afforded a red solid of **1** in 26% yield (0.247 g).

2.3. *Reaction of $Fe_3(CO)_{12}$ and Ph_2PH in the presence of Et_3N*

A 100-mL Schlenk flask equipped with a stir bar and serum cap was charged with 15 mL of THF, 0.94 g (5 mM) of Ph_2PH, 0.7 mL (5 mM) of Et_3N, and cooled to 0 °C. To this stirred solution was added 2 g (4 mM) of $Fe_3(CO)_{12}$. After 1 min of stirring, the solvent was removed in vacuo and the resulting residue was chromatographed by TLC on silica gel. Elution with petroleum ether/acetone (v/v, 1 : 12) gave yellow, orange-yellow and orange-red bands in the order of decreasing R_f values. The orange-red band afforded red crystals of **1** after recrystallization from deoxygenated petroleum ether (60–90 °C) and CH_2Cl_2, m.p. 121–123 °C, in 25% yield (0.61 g). The orange-yellow band offered orange-red crystals of **2** after recrystallization from deoxygenated petroleum ether (60–90 °C) and CH_2Cl_2, m.p. 132–134 °C, in 14% yield (0.228 g). The yellow band provided yellow crystals of **3** after recrystallization from deoxygenated petroleum ether (60–90 °C) and CH_2Cl_2, m.p. 188.3–188.9 °C (lit.: 178–179 °C [39]; 186–188 (dec.) °C [40]), in 19% yield (0.307 g).

In **1**, Anal. Calcd for $C_{18}H_{11}Fe_2O_7P$ (%): C, 44.86; H, 2.30; found: C, 44.65; H, 2.47. IR (KBr disk): ν(OH) 3544.90 (m); ν(C≡O) 2066.51 (s), 2029.67 (vs), 1966.48 (vs) cm^{-1}. ^1H NMR (600 MHz, $CDCl_3$, TMS): δ −2.931 (d, $^3J_{H\text{-}P} = 11.4$ Hz, 1H, OH), 7.365–7.408, 7.408–7.444, 7.477–7.509, 7.696–7.727 (4m, 5H, 1H, 2H, 2H, $2C_6H_5$). ^{13}C NMR (150.928 MHz, $CDCl_3$, TMS): δ 128.522, 128.592, 128.927, 128.992, 130.302 (d, $J = 3.17$ Hz), 130.661 (d, $J = 2.87$ Hz), 133.496, 133.555, 134.591, 134.644 ($2C_6H_5$), 209.392 (s, 6C≡O). ^{31}P NMR (242.98 MHz, $CDCl_3$, 85% H_3PO_4): δ 122.181 (d, $^3J_{P\text{-}H} = 10.69$ Hz).

In **2**, Anal. Calcd for $C_{30}H_{20}Fe_2O_7P_2$ (%): C, 54.09; H, 3.03; found: C, 54.21; H, 3.25. IR (KBr disk): ν(C≡O) 2065.70 (s), 2020.63 (vs), 1995.55 (s), 1958.83 (s) cm^{-1}. ^1H NMR (600 MHz, $CDCl_3$, TMS): δ 6.690–6.721, 6.779–6.809, 6.861–6.913, 6.978–7.001, 7.290–7.375, 7.461–7.479, 7.582–7.613, 7.819–7.848 (8 m, 2H, 2H, 3H, 1H, 6H, 2H, 2H, 2H, $4C_6H_5$). ^{13}C NMR (150.928 MHz, $CDCl_3$, TMS): δ 125.934 (d, $J = 10.87$ Hz), 126.438 (d, $J = 14.41$ Hz), 127.069, 127.128, 127.193, 127.299, 127.601 (d, $J = 9.21$ Hz), 128.426, 128.879 (d, $J = 14.64$ Hz), 132.141 (d, $J = 7.39$ Hz), 132.963 (d, $J = 6.79$ Hz), 134.932, 135.106, 139.434, 139.673, 141.517, 141.798, 142.312, 142.644 ($4C_6H_5$), 208.148, 208.663, 208.782, 209.709, 209.992, 211.228 (6C≡O). ^{31}P NMR (242.98 MHz, $CDCl_3$, 85% H_3PO_4): δ 178.037 (d, $^2J_{P\text{-}P} = 57.10$ Hz, PPh_2), 100.731 (d, $^2J_{P\text{-}P} = 57.10$ Hz, $OPPh_2$).

In **3**, Anal. Calcd for $C_{30}H_{20}Fe_2O_6P_2$ (%): C, 55.42; H, 3.10; found: C, 55.33; H, 3.07. IR (KBr disk): ν(C≡O) 2055.63 (s), 2016.85 (s), 1983.18 (s), 1961.21 (vs) cm^{-1}. ^1H NMR (600 MHz, $CDCl_3$, TMS): δ 6.684–6.709, 6.797–6.821, 7.092–7.124, 7.214–7.270, 7.560–7.589 (t, t, q, m, q, 4H, 2H, 4H, 6H, 4H, $4C_6H_5$). ^{13}C NMR (150.928 MHz, $CDCl_3$, TMS): δ 127.985 (d, $J = 4.98$ Hz), 128.019 (d, $J = 5.28$ Hz), 128.407 (d, $J = 3.47$ Hz), 128.439 (d, $J = 4.83$ Hz), 128.854 (s), 129.679 (s), 133.096 (d, $J = 3.62$ Hz), 133.121 (d, $J = 3.77$ Hz), 133.751 (d, $J = 4.08$ Hz), 133.777 (d, $J = 3.77$ Hz) ($4C_6H_5$), 212.903 (t, $^2J_{C\text{-}P} = 4.53$ Hz, 6C≡O). ^{31}P NMR (242.98 MHz, $CDCl_3$, 85% H_3PO_4): δ 142.441(s).

2.4. *Reaction of $Fe_3(CO)_{12}$ and Ph_2PH*

A 100-mL Schlenk flask equipped with a stir bar and serum cap was charged with 15 mL of THF, 0.376 g (2 mM) of Ph_2PH, and 1.007 g (2 mM) of $Fe_3(CO)_{12}$. After 24 h of stirring, the solvent was removed under reduced pressure; the resulting residue was chromatographed by TLC on silica gel. Elution with petroleum ether/acetone (v/v, 1 : 20) gave an orange-red band from which red crystals of **1** were obtained in 45% yield (0.445 g) after recrystallization from deoxygenated petroleum ether (60–90 °C) and CH_2Cl_2.

2.5. *Influence of O_2 and H_2O on the reaction of $Fe_3(CO)_{12}$ and Ph_2PH*

After THF standing in air for 1 h and 0.5 mL of H_2O added, the reaction of $Fe_3(CO)_{12}$ and Ph_2PH afforded **1** in 15% yield with trace amounts of **2** and **3**. Using deoxygenated THF, H_2O (0.5 mL) was added, the reaction of $Fe_3(CO)_{12}$ and Ph_2PH offered **1** in 24% yield, with trace amounts of **2** and **3**. Using deoxygenated THF with 0.1 mL of H_2O added, the reaction of $Fe_3(CO)_{12}$ and Ph_2PH gave **1** in 49% yield with trace amounts of **2** and **3**.

2.6. *X-ray structure determinations of complexes*

Single crystals of **1–3** suitable for X-ray diffraction analyses were grown by slow evaporation of the CH_2Cl_2-petroleum ether solutions of **1–3** at 0–4 °C. For each complex, a selected single crystal was mounted on a Bruker APEX II CCD diffractometer using graphite-monochromated Mo-Kα radiation ($\lambda = 0.71073$ Å) at 296 K. Data collection and reduction were performed using SAINT software. An empirical absorption correction was applied using SADABS. The structures were solved by direct methods using the SIR-2004 software and refined by full-matrix least-squares on F^2 with anisotropic thermal parameters for all non-hydrogen atoms using the SHELXTL package [41, 42]. All hydrogens attached to carbon in **1–3** were placed at geometrically idealized positions and subsequently treated as riding with C–H = 0.93 (aromatic) Å and U_{iso}(H) values of $1.2U_{eq}$(C). For **1**, hydrogen bonded to oxygen was located from the difference Fourier map and refined isotropically with U_{iso}(H) of $1.5U_{eq}$(O). Platon views of complexes were drawn using PWT software [43]. Details of crystal data, data collections, and structure refinements are summarized in table 1.

2.7. *Electrochemical determinations of complexes*

Cyclic voltammograms (CV) were obtained by using a 3-electrode cell with a glassy carbon 3 mm diameter working electrode, platinum plate counter electrode, and SCE reference electrode. The electrolyte solution for all experiments was 0.100 M $^nBu_4NPF_6$ in MeCN. The potentials (E) at the working electrode in all CV's are reported with respect to the ferrocenium/ferrocene couple in electrolyte solution. The ferrocenium/ferrocene coupling data were collected at the end of each experiment. All CV's reported are background-corrected, i.e. the scan with only electrolyte present was subtracted from the raw data. All background scans confirmed sufficient removal of O_2 as seen by the absence of a reduction peak at ca. −1.2 V. CV data were collected under flow of N_2 gas.

Table 1. Crystal data, data collections, and structure refinements for **1–3**.

	1	**2**	**3**
Formula	$C_{18}H_{11}Fe_2O_7P$	$C_{60}H_{40}Fe_4O_{14}P_4{\cdot}CH_2Cl_2$	$C_{30}H_{20}Fe_2O_6P_2{\cdot}CH_2Cl_2$
M_r	481.94	1417.13	735.03
Cryst system	Triclinic	Triclinic	Monoclinic
Space group	$P\bar{1}$	$P\bar{1}$	$P2_1/m$
a (Å)	9.9129(12)	11.8204(15)	11.3318(12)
b (Å)	9.9866(12)	16.9649(11)	12.7182(14)
c (Å)	12.2975(14)	17.1472(14)	11.8256(13)
α (°)	96.5898(10)	65.974(3)	90
β (°)	106.860(2)	89.2813(12)	106.161(4)
γ (°)	118.474(3)	84.8664(16)	90
V (Å^3)	976.7(2)	3127.0(5)	1637.0(3)
Z	2	2	2
D_{Calcd} (g cm^{-3})	1.639	1.505	1.491
μ (mm^{-1})	1.604	1.160	1.188
F (0 0 0)	484	1436	744
Index ranges	$-13 \le h \le 12$	$-15 \le h \le 15$	$-14 \le h \le 14$
	$-13 \le k \le 12$	$-22 \le k \le 17$	$-16 \le k \le 16$
	$-16 \le l \le 15$	$-22 \le l \le 22$	$-15 \le l \le 15$
Reflections measured	20,090	33,564	25,268
Unique reflections	4563	14,091	3925
Reflections ($I > 2\sigma(I)$)	3264	7795	2844
R_{int}	0.0741	0.0532	0.0516
$2\theta_{max}$ (°)	55.8	55.2	55.0
R	0.0459	0.0625	0.0479
R_w	0.1204	0.1465	0.1273
GooF	1.02	1.02	1.04
Largest diff. peak and hole (e Å^{-3})	0.62/−0.58	0.57/−0.50	1.08/−0.89

3. Results and discussion

3.1. *Syntheses of complexes*

In order to develop the synthetic methodologies of Fe/S cluster complexes [44–49], we have explored the reaction of $Fe_3(CO)_{12}$ and Ph_2PSH *in situ* generated from Ph_2PH and elemental sulfur in the presence of Et_3N with PhCOCl. This reaction afforded **1**, [$Fe_2(CO)_6$(μ-PPh_2)(μ-OH)], rather than an expected complex, [$Fe_2(CO)_6$(μ-k^{2}P,S-Ph_2PS)(μ-COPh)]. In view of scarce μ-OH-containing complexes [50] and the important function of the μ-OH ligand in hydrogenases [51], we have carried out the reaction of $Fe_3(CO)_{12}$, Ph_2PH, and Et_3N in the absence of PhCOCl. This reaction offered $Fe_2(CO)_6$(μ-PPh_2)(μ-L) (**1**, L = OH; **2**, L = $OPPh_2$; **3**, L = PPh_2) (scheme 1). THF was not deoxygenated by bubbling N_2 for 15 min before use and Et_3N was used as received. As mentioned below, if oxygen and water were strictly excluded, **1** and **2** could not be obtained.

In order to increase the yield of **1** and to understand the role of Et_3N, we have performed the following experiments: (1) the reaction of $Fe_3(CO)_{12}$ and Ph_2PH in the presence of H_2O; (2) the reaction of $Fe_3(CO)_{12}$, Ph_2PH, and H_2O in the presence of Et_3N; and (3) the above reactions under strict O_2-free conditions [52]. These experiments confirm that Et_3N as a Lewis base shortens the reaction time from 24 h to 1 min. The absence of O_2 can hinder formation of **2**. However, excess O_2 can lead to disappointing results. The presence of H_2O (1–5 eq) can increase the yield of **1** up to 49%.

Particularly, so far, three examples with the μ-OH ligand have appeared in the literature [50]: $Fe_2(CO)_6[P(p\text{-}C_6H_4CH_3)_2]OH$ was generated from deprotonation of

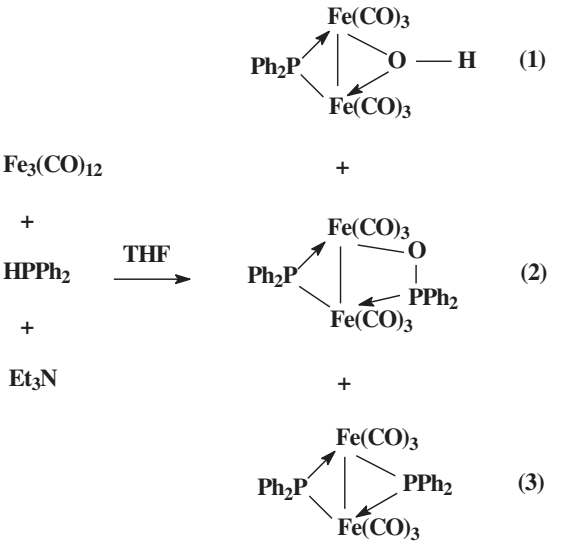

Scheme 1. Syntheses of **1–3**.

$Fe(CO)_4[P(p\text{-}C_6H_4CH_3)_2]H$ with BuLi and subsequently treated with $Fe_2(CO)_9$ [53]; $Fe_2(CO)_6[\mu\text{-}PHCH(SiMe_3)_2](\mu\text{-}OH)$ was obtained as one of the products in the reaction of $[NEt_4]_2[Fe_2(CO)_8]$ with $Cl_2PCH(SiMe_3)_2$ [54]; $Fe_2(CO)_4(\mu\text{-}PPh_2)(\mu\text{-dppm})(\mu\text{-}OH)$ resulted from slow oxidation of $Fe_2(CO)_4(\mu\text{-}PPh_2)(\mu\text{-}PPh_2CH_2PPh_2)(\mu\text{-CO})(\mu\text{-H})$ on alumina [55]. The direct route to μ-OH-containing diiron complexes has been discovered by us (Equation (1)).

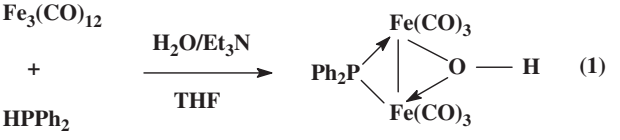

Synthesis of **1**.

To our knowledge, **2** with the $\mu\text{-}OPPh_2$ ligand is unprecedented although Pd, Pt, and Re complexes with $\mu\text{-}OPPh_2$, $\mu\text{-}OPCy_2$, and $\mu\text{-}OPBu^t{}_2$ ligands have been reported [56–59].

Complex **3** was first prepared by Job *et al.* [39] from pentacarbonyl iron and tetraphenylphosphine at 220 °C, which cannot be conveniently performed on a large scale. Collman *et al.* [40] then developed an alternative synthesis of **3** via diphenylchlorophosphine and disodium octacarbonyldiferrate. Ballinas-López *et al.* [60] reported a third synthesis via diphenylphosphine and dodecacarbonyltriiron at 120 °C in a sealed ampoule for 24 h. Strangely, **3** has not been completely characterized by these authors.

3.2. *X-ray structures of 1–3*

Structures of the above complexes have been determined by X-ray crystallography. Selected geometric parameters have been listed in table 2. The X-ray crystallographic study of **1**

Table 2. Selected geometric parameters (Å, °) for **1–3**.

1		**2a**		**2b**		**3**	
Fe1–Fe2	2.5127(7)	Fe1–Fe2	2.6542(7)	Fe3–Fe4	2.6445(8)	Fe1–Fe1^{i}	2.6047(9)
Fe1–P1	2.2263(9)	Fe1–P1	2.2190(11)	Fe3–P3	2.2216(12)	Fe1–P1	2.2194(9)
Fe2–P1	2.2338(9)	Fe2–P1	2.2253(11)	Fe4–P3	2.2238(11)	Fe1–P2	2.2276(10)
Fe1–O7	1.963(2)	Fe1–P2	2.8074(10)	Fe3–P4	2.8101(12)		
Fe2–O7	1.964(2)	Fe2–P2	2.2625(11)	Fe4–P4	2.2598(12)		
O7–H7O	0.813(10)	Fe1–O7	2.022(2)	Fe3–O14	2.035(2)		
		P2–O7	1.555(2)	P4–O14	1.534(3)		
		Fe1–P1–Fe2	73.34(4)	Fe3–P4–Fe4	73.01(4)		
Fe1–P1–Fe2	68.58(3)	Fe2–P2–O7	105.55(9)	Fe4–P4–O14	105.68(11)	Fe1–P1–Fe1^{i}	71.86(4)
Fe1–O7–Fe2	79.56(9)	Fe1–O7–P2	102.65(13)	Fe3–O14–P4	103.00(14)	Fe1–P2–Fe1^{i}	71.55(4)

^{i}Symmetry code: x, $-y+1/2$, z.

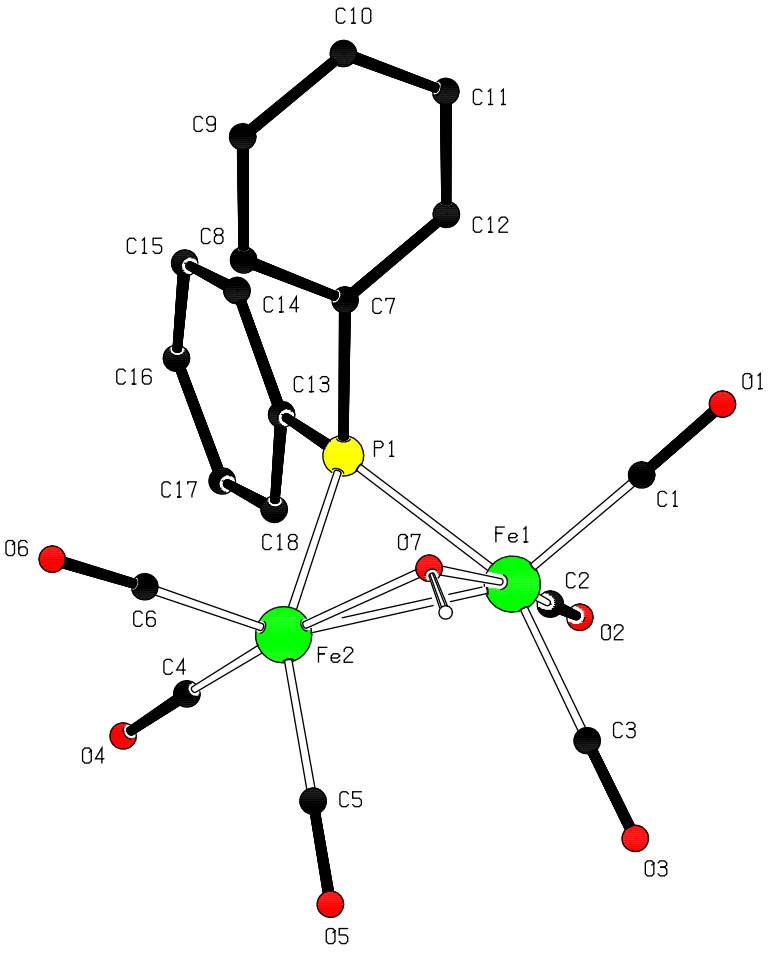

Figure 1. X-ray crystal structure of **1**.

reveals that it exists as a discrete dinuclear molecule in which the irons are linked by PPh_2 and OH groups (figure 1).

The Fe–Fe bond distance of 2.5127(7) Å is close to that found (2.511(2) Å) in $Fe_2(CO)_6[\mu\text{-}P(p\text{-}C_6H_4CH_3)_2](\mu\text{-OH})$ [53] but markedly shorter than those in **2–3** (see below). Also, the Fe–P bond distances of 2.2263(9) and 2.2338(9) Å are very close to those observed (2.236(3) and 2.239(3) Å) in the reported complex. The OH group bridges the two Fe ions symmetrically, with the Fe–O distances of 1.963(2) and 1.964(2) Å, and Fe–O–Fe angle of 79.56(9)°. The H–O···P angle of 170(3)° indicates that **1** exists as an equatorial rather than an axial isomer [45, 49].

Unlike **1**, **2** with two different molecules (**2a** and **2b**) crystallizes in the $P\bar{1}$ space group (figure 2). In **2a** and **2b**, the $OPPh_2$ via O and P links two iron ions in a σ,n-mode, with bond distances of 2.6542(7) (Fe1–Fe2), 2.2625(11) (Fe2–P2), 2.022(2) (Fe1–O7), and 1.555(2) (P2–O7) Å for **2a** and 2.6445(8) (Fe3–Fe4), 2.2598(12) (Fe4–P4), 2.035(2) (Fe3–O14), and 1.534(3) (P4–O14) Å for **2b**. The P–O bond distances are close to 1.536(4) Å in $[Pd(\mu\text{-}OPPh_2)(N(Me)C(O)N(Me)PPh_2)]_2$ and 1.556(4) Å in $(PHCy_2)_2Pt_2(\mu\text{-}PCy_2)(\mu\text{-}OPCy_2)$,

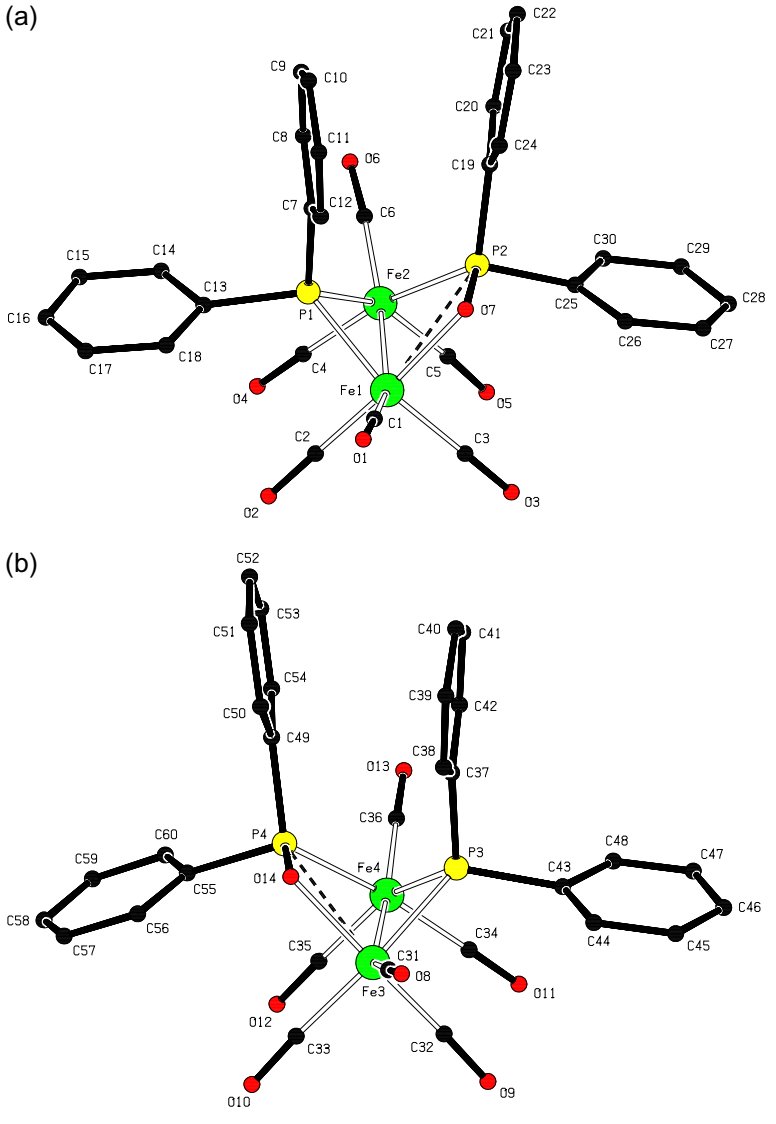

Figure 2. X-ray crystal structure of **2** (up, **2a**; down, **2b**). Dashed lines represent intramolecular Fe···P contacts.

in agreement with a P–O single bond [57, 58]. Noteworthy is that the distances of 2.8074 (10) (Fe1–P2) and 2.8101(12) (Fe3–P4) Å indicate the presence of strong intramolecular contacts between Fe and P in **2**, because these are significantly shorter than the sum of the van der Waals radii of iron and phosphorus [R(Fe) + R(P) = 3.91 Å].

As reported by Ballinas-López *et al.* [60], **3** with solvent CH_2Cl_2 crystallizes in the $P2_1/m$ space group (figure 3). The molecule of **3** lies across a mirror plane. Two PPh_2 ligands bridge two $Fe(CO)_3$ units to form a dinuclear complex, in which the Fe–Fe distance is 2.6047(9) Å and almost equal to 2.6071(6) Å reported by Ballinas-López *et al.* The P2–Fe1–Fe1i–P1 ring adopts a butterfly arrangement with the P-donor in the wingtip positions [code: (i) x, $-y+1/2$, z]. The dihedral angle between the two Fe–P–Fe planes is 75.03(6)°.

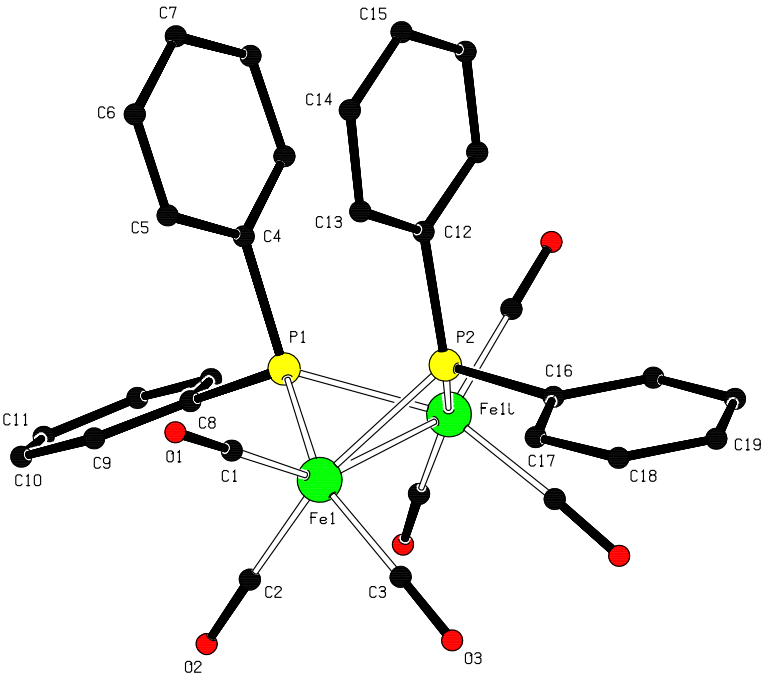

Figure 3. X-ray crystal structure of **3** (symmetry code: (i) x, $-y+1/2$, z).

The Fe–P bond distances and Fe–P–Fe bond angles are comparable to those (2.2250(9), 2.2200(8) Å; 71.73(3)°, 71.91(3)°) observed by Ballinas-López *et al.*

3.3. *Spectroscopic analysis of 1–3*

The above complexes have also been characterized by elemental analyses and spectroscopies. As indicated in figures 1–3, their IR spectra show characteristic absorption bands at 1958–2067 cm^{-1} for their terminal CO ligands. Additionally, the OH group appears at 3545 cm^{-1} for **1**, indicating that it does not act as a hydrogen bonding donor which is in agreement with the X-ray diffraction analysis of **1**.

The ^{1}H NMR spectra of all complexes display the corresponding signals for their phenyl groups. Particularly, for **1**, the OH group which is confirmed by D_2O exchange, exhibits a doublet with a $^{3}J_{H\text{-}P}$ coupling constant of 11.40 Hz at −2.931 ppm. The ^{31}P NMR spectra show a doublet with a $^{3}J_{H\text{-}P}$ coupling constant of 10.69 Hz at 122.181 ppm for **1**, two doublets with a $^{2}J_{P\text{-}P}$ coupling constant of 57.10 Hz at 178.037 ppm (PPh_2) and 100.731 ppm ($OPPh_2$) for **2** and a singlet at 142.441 ppm for **3**. In the $^{13}C\{^{1}H\}$ NMR spectra, **1** shows only a singlet at 209.128 ppm corresponding to terminal carbonyl C, suggesting that the carbonyl ligands are undergoing rapid exchange between two Fe atoms on the NMR time scale at room temperature [44–49]. Terminal carbonyls of **2** are six singlets at 208.148, 208.663, 208.782, 209.709, 209.992, and 211.228 ppm. However, **3** exhibits an expected triplet (with a $^{2}J_{C\text{-}P}$ coupling constant of 4.53 Hz at 212.903 ppm). Therefore, except for fluxionality of CO site-exchanges in their solutions, spectroscopic data are in accordance with the above X-ray diffraction analyses.

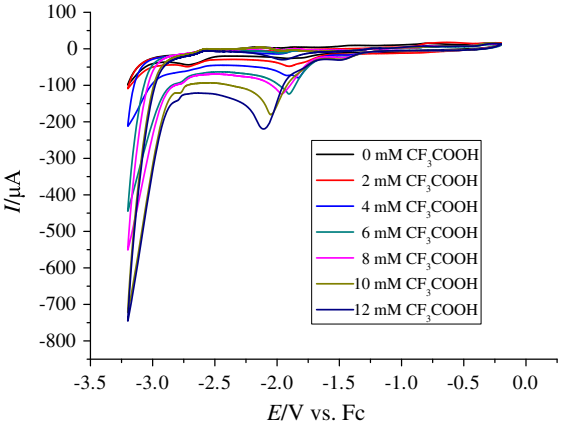

Figure 4. CV of **1** (1.0 mM) with CF_3CO_2H (0–12 mM) in 0.1 M n-Bu_4NPF_6/MeCN at a scan rate of 100 mV s^{-1}.

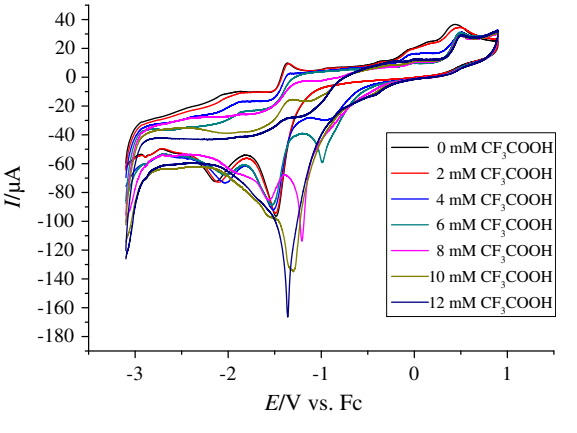

Figure 5. CV of **2** (1.0 mM) with CF_3CO_2H (0–12 mM) in 0.1 M n-Bu_4NPF_6/MeCN at a scan rate of 100 mV s^{-1}.

3.4. *Electrochemistry of complexes*

In order to examine whether the above complexes could act as electrocatalysts for proton reduction to hydrogen, we have investigated their electrochemical properties in the presence or absence of CF_3CO_2H under CV conditions. CV was carried out in MeCN/Bu_4NPF_6 solutions to identify the electrochemically induced oxidation and reduction processes. In MeCN, CV of **1** shows two irreversible reduction waves at −1.837 and −2.690 V (figure 4). For each step, the peak current varies as the square root of the scan rate in the measured range, consistent with a fast diffusion limited electron transfer (figure S13, see online supplemental material at http://dx.doi.org/10.1080/00958972.2014.940925).

CV of **2** displays two irreversible oxidation waves at 0.432 and −1.358 V and two irreversible reduction waves at −1.483 and −2.133 V (figure 5). For each step, the peak current varies as the square root of the scan rate in the measured range, consistent with a fast diffusion limited electron transfer (figure S15).

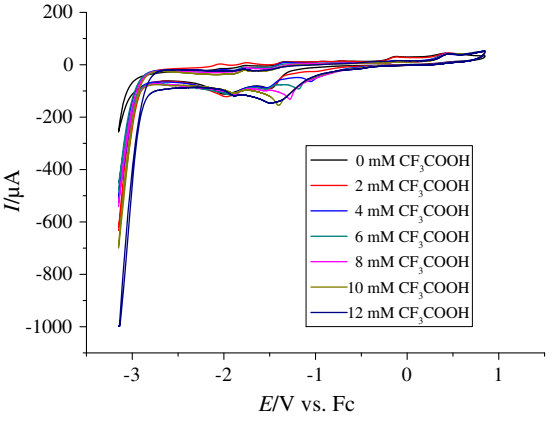

Figure 6. CV of **3** (1.0 mM) with CF_3CO_2H (0–12 mM) in 0.1 M n-Bu_4NPF_6/MeCN at a scan rate of 100 mV s^{-1}.

Table 3. Redox potentials (*V*) of **1**–**3** referenced against Fc^+/Fc in MeCN.

Complex	E_p^{ox1}	E_p^{ox2}	E_p^{red1}	E_p^{red2}
1			−1.837	−2.690 (0.38)[†]
2	0.432	−1.358	−1.483 (0.14)	−2.133
3			−1.496 (0.13)	−1.982

[†]$CE = (i_{cat}/i_d)/(C_{HA}/C_{cat})$: W for $0 < CE < 0.25$, M for $0.25 < CE < 0.75$ and S for $CE > 0.75$.

As in **1**, **3** exhibits two irreversible reduction waves at −1.496 and −1.982 V (figures 6 and S16).

According to a criterion of catalytic efficiency ($CE = (i_{cat}/i_d)/(C_{HA}/C_{cat})$, where i_{cat} is the catalytic current, i_d is the current for reduction of the catalyst in the absence of acid, C_{HA} is the acid concentration and C_{cat} is the catalyst concentration) proposed by Lichtenberger *et al.* [14], as listed in table 3, **1** shows medium CE at the second reduction wave, whereas **2** and **3** exhibit weak CE at the first reduction wave [61, 62]. Therefore, this type of complex containing the bridging hydroxyl group will be of interest to further investigate hydrogenase models.

4. Conclusion

Three complexes, $Fe_2(CO)_6(\mu\text{-}PPh_2)(\mu\text{-L})$ (**1**, L = OH; **2**, L = $OPPh_2$; **3**, L = PPh_2), have been synthesized by reaction of $Fe_3(CO)_{12}$ and Ph_2PH in the presence of Et_3N. The reaction conditions generating **1** have been optimized. Et_3N acting as a Lewis base can largely shorten the reaction time. The presence of H_2O can increase the yield of **1**. Electrochemical studies confirm that they show catalytic H_2-producing activities.

Supplementary material

CCDC 978089–978092 contain the supplementary crystallographic data (including structure factors) for this paper. These data can be obtained free of charge from The Cambridge Crystallographic Data Center via www.ccdc.cam.ac.uk/data_request/cif.

Funding

We are grateful to the Mao Zedong Foundation of China, Project funded by the Priority Academic Program Development of Jiangsu Higher Education Institutions (PAPD), Natural Science Foundation of China [grant number 20572091] and Natural Science Foundation of Jiangsu Province [grant number 05KJB150151] for financial support of this work.

References

[1] M. Balat. *Int. J. Hydrogen Energy*, **33**, 4013 (2008).
[2] N.Z. Muradov, T.N. Veziroglu. *Int. J. Hydrogen Energy*, **33**, 6804 (2008).
[3] G.J. Kubas. *J. Organomet. Chem.*, **694**, 2648 (2009).
[4] N.S. Lewis, D.G. Nocera. *Proc. Natl. Acad. Sci. USA*, **103**, 15729 (2006).
[5] S.C. Marinescu, J.R. Winkler, H.B. Gray. *Proc. Natl. Acad. Sci. USA*, **109**, 15127 (2012).
[6] S. Ogo. *Chem. Commun.*, **45**, 3317 (2009).
[7] (a) C. Tard, C.J. Pickett. *Chem. Rev.*, **109**, 2245 (2009); (b) T.R. Simmons, G. Berggren, M. Bacchi, M. Fontecave, V. Artero. *Coord. Chem. Rev.*, **270–271**, 127 (2014).
[8] F. Gloaguen, T.B. Rauchfuss. *Chem. Soc. Rev.*, **38**, 100 (2009).
[9] M. Rakowski DuBois, D.L. DuBois. *Chem. Soc. Rev.*, **38**, 62 (2009).
[10] I.P. Georgakaki, L.M. Thomson, E.J. Lyon, M.B. Hall, M.Y. Darensbourg. *Coord. Chem. Rev.*, **238–239**, 255 (2003).
[11] L.-C. Sun, B. Åkermark, S. Ott. *Coord. Chem. Rev.*, **249**, 1653 (2005).
[12] (a) J.-F. Capon, F. Gloaguen, F.Y. Pétillon, P. Schollhammer, J. Talarmin. *Eur. J. Inorg. Chem.*, **2008**, 4671 (2008); (b) P.-H. Zhao, X.-H. Li, Y.-F. Liu, Y.-Q. Liu. *J. Coord. Chem.*, **67**, 766 (2014).
[13] J.-F. Capon, F. Gloaguen, F.Y. Pétillon, P. Schollhammer, J. Talarmin. *Coord. Chem. Rev.*, **253**, 1476 (2009).
[14] G.A.N. Felton, C.A. Mebi, B.J. Petro, A.K. Vannucci, D.H. Evans, R.S. Glass, D.L. Lichtenberger. *J. Organomet. Chem.*, **694**, 2681 (2009).
[15] B.E. Barton, M.T. Olsen, T.B. Rauchfuss. *J. Am. Chem. Soc.*, **130**, 16834 (2008).
[16] S. Löscher, L. Schwartz, M. Stein, S. Ott, M. Haumann. *Inorg. Chem.*, **46**, 11094 (2007).
[17] L. Schwartz, G. Eilers, L. Eriksson, A. Gogoll, R. Lomoth, S. Ott. *Chem. Commun.*, 520 (2006).
[18] P. Das, J.-F. Capon, F. Gloaguen, F.Y. Pétillon, P. Schollhammer, J. Talarmin, K.W. Muir. *Inorg. Chem.*, **43**, 8203 (2004).
[19] S. Ott, M. Kritikos, B. Åkermark, L.-C. Sun, R. Lomoth. *Angew. Chem. Int. Ed.*, **43**, 1006 (2004).
[20] J.-F. Capon, S. Ezzaher, F. Gloaguen, F.Y. Pétillon, P. Schollhammer, J. Talarmin, T.J. Davin, J.E. McGrady, K.W. Muir. *New J. Chem.*, **31**, 2052 (2007).
[21] J.-F. Capon, F. Gloaguen, P. Schollhammer, J. Talarmin. *J. Electroanal. Chem.*, **566**, 241 (2004).
[22] S.J. Borg, T. Behrsing, S.P. Best, M. Razavet, X.-M. Liu, C.J. Pickett. *J. Am. Chem. Soc.*, **126**, 16988 (2004).
[23] L.-C. Song, C.-G. Li, J.-H. Ge, Z.-Y. Yang, H.-T. Wang, J. Zhang, Q.-M. Hu. *J. Inorg. Biochem.*, **102**, 1973 (2008).
[24] J.-F. Capon, F. Gloaguen, P. Schollhammer, J. Talarmin. *J. Electroanal. Chem.*, **595**, 47 (2006).
[25] L. Schwartz, P.S. Singh, L. Eriksson, R. Lomoth, S. Ott. *C. R. Chimie*, **11**, 875 (2008).
[26] Y.-C. Liu, K.-T. Chu, R.-L. Jhang, G.-H. Lee, M.-H. Chiang. *Chem. Commun.*, **49**, 4743 (2013).
[27] G.A.N. Felton, A.K. Vannucci, J.Z. Chen, L.T. Lockett, N. Okumura, B.J. Petro, U.I. Zakai, D.H. Evans, R.S. Glass, D.L. Lichtenberger. *J. Am. Chem. Soc.*, **129**, 12521 (2007).
[28] P.I. Volkers, T.B. Rauchfuss. *J. Inorg. Biochem.*, **101**, 1748 (2007).
[29] P.-Y. Orain, J.-F. Capon, F. Gloaguen, P. Schollhammer, J. Talarmin. *Int. J. Hydrogen Energy*, **35**, 10797 (2010).
[30] M.H. Cheah, S.J. Borg, S.P. Best. *Inorg. Chem.*, **46**, 1741 (2007).
[31] M.H. Cheah, S.J. Borg, M.I. Bondin, S.P. Best. *Inorg. Chem.*, **43**, 5635 (2004).
[32] M.K. Harb, T. Niksch, J. Windhager, H. Görls, R. Holze, L.T. Lockett, N. Okumura, D.H. Evans, R.S. Glass, D.L. Lichtenberger, M. El-khateeb, W. Weigand. *Organometallics*, **28**, 1039 (2009).
[33] M.K. Harb, J. Windhager, T. Niksch, H. Görls, T. Sakamoto, E.R. Smith, R.S. Glass, D.L. Lichtenberger, D.H. Evans, M. El-khateeb, W. Weigand. *Tetrahedron*, **68**, 10592 (2012).
[34] M.K. Harb, U.-P. Apfel, J. Kübel, H. Görls, G.A.N. Felton, T. Sakamoto, D.H. Evans, R.S. Glass, D.L. Lichtenberger, M. El-khateeb, W. Weigand. *Organometallics*, **28**, 6666 (2009).
[35] L.-C. Song, B. Gai, Z.-H. Feng, Z.-Q. Du, Z.-J. Xie, X.-J. Sun, H.-B. Song. *Organometallics*, **32**, 3673 (2013).
[36] R. Zaffaroni, T.B. Rauchfuss, A. Fuller, L. De Gioia, G. Zampella. *Organometallics*, **32**, 232 (2013).
[37] R.B. King. *Organometallic Syntheses: Transition-Metal Compounds*, Academic Press, New York (1965).
[38] Z. Rohlík, P. Holzhauser, J. Kotek, J. Rudovský, I. Němec, P. Hermann, I. Lukeš. *J. Organomet. Chem.*, **691**, 2409 (2006).
[39] B.E. Job, R.A.N. Mclean, D.T. Thompson. *Chem. Commun. (London)*, 895 (1966).

[40] J.P. Collman, R.K. Rothrock, R.G. Finke, E.J. Moore, F. Rose-Munch. *Inorg. Chem.*, **21**, 146 (1982).
[41] M.C. Burla, R. Caliandro, M. Camalli, B. Carrozzini, G.L. Cascarano, L. De Caro, C. Giacovazzo, G. Polidori, R. Spagna. *J. Appl. Crystallogr.*, **38**, 381 (2005).
[42] G.M. Sheldrick. *Acta Crystallogr.*, **A64**, 112 (2008).
[43] A.L. Spek. *Acta Crystallogr.*, **D65**, 148 (2009).
[44] Y.-C. Shi, H. Tan, Y. Shi. *Polyhedron*, **67**, 218 (2014).
[45] Y.-C. Shi, F. Gu. *Chem. Commun.*, **49**, 2255 (2013).
[46] Y.-C. Shi, H.-R. Cheng, Q. Fu, F. Gu, Y.-H. Wu. *Polyhedron*, **56**, 160 (2013).
[47] (a) Y.-C. Shi, Q. Fu. *Z. Anorg. Allg. Chem.*, **639**, 1791 (2013); (b) W. Yang, Q. Fu, J. Zhao, H.-R. Cheng, Y.-C. Shi. *Acta Crystallogr.*, **C70**, 528 (2014).
[48] Y.-C. Shi, H.-R. Cheng, D.-C. Cheng. *Acta Crystallogr.*, **C69**, 581 (2013).
[49] Y.-C. Shi, H.-R. Cheng, H. Tan. *J. Organomet. Chem.*, **716**, 39 (2012).
[50] H.W. Roesky, S. Singh, K.K.M. Yusuff, J.A. Maguire, N.S. Hosmane. *Chem. Rev.*, **106**, 3813 (2006).
[51] (a) Y. Ohki, K. Yasumura, K. Kuge, S. Tanino, M. Ando, Z. Li, K. Tatsumi. *Proc. Natl. Acad. Sci. USA*, **105**, 7652 (2008); (b) D.M. Heinekey. *J. Organomet. Chem.*, **694**, 2671 (2009).
[52] O.V. Ozerov. *Chem. Soc. Rev.*, **38**, 83 (2009).
[53] P.M. Treichel, W.K. Dean, J.C. Calabrese. *Inorg. Chem.*, **12**, 2908 (1973).
[54] A.M. Arif, A.H. Cowley, M. Pakulski, M.A. Pearsall, W. Clegg, N.C. Norman, A.G. Orpen. *J. Chem. Soc., Dalton Trans.*, 2713 (1988).
[55] (a) G. Hogarth, M.H. Lavender. *J. Chem. Soc., Dalton Trans.*, 143 (1993); (b) B. Walther, H. Hartung, H.-C. Böttcher, U. Baumeister, U. Böhland, J. Reinhold, J. Sieler, J. Ladriere, H.M. Schiebel. *Polyhedron*, **10**, 2423 (1991).
[56] N.W. Alcock, P. Bergamini, T.M. Gomes-Carniero, R.D. Jackson, J. Nicholls, A.G. Orpen, P.G. Pringle, S. Sostero, O. Traverso. *J. Chem. Soc., Chem. Commun.*, 980 (1990).
[57] A.M.Z. Slawin, M. Wainwright, J.D. Woollins. *J. Chem. Soc., Dalton Trans.*, 2724 (2001).
[58] V. Gallo, M. Latronico, P. Mastrorilli, C.F. Nobile, F. Polini, N. Re, U. Englert. *Inorg. Chem.*, **47**, 4785 (2008).
[59] R.D. Adams, B. Captain, P.J. Pellechia. *Organometallics*, **26**, 6564 (2007).
[60] M.G. Ballinas-López, I.I. Padilla-Martínez, F.J. Martínez-Martínez, H. Höpfl, E.V. García-Báez. *Acta Crystallogr.*, **E61**, m1475 (2005).
[61] F. Gloaguen, J.D. Lawrence, T.B. Rauchfuss. *J. Am. Chem. Soc.*, **123**, 9476 (2001).
[62] L.-C. Song, C.-G. Li, J. Gao, B.-S. Yin, X. Luo, X.-G. Zhang, H.-L. Bao, Q.-M. Hu. *Inorg. Chem.*, **47**, 4545 (2008).